Computational Fluid Dynamics Optimization of a Heat Exchanger Design for Photovoltaic Thermal Retrofit Applications

Abel Climente García[1], Damu Murali[2], Iván P. Acosta-Pazmiño[1], María Herrando[3], Mario Morales-Hernández[4], Juan Pablo Santana [2] and João Gomes[2]

[1] MG Sustainable Engineering AB, Uppsala (Sweden)

[2] Department of Building Engineering, Energy Systems and Sustainable Science, University of Gävle, Gävle (Sweden)

[3] Instituto Tecnológico de Aragón (ITA), Zaragoza (Spain)

[4] Fluid Dynamics Technology Group, I3A, University of Zaragoza, Zaragoza (Spain)

Abstract

This paper investigates the geometrical optimization of a heat exchanger designed for retrofitting photovoltaic (PV) panels into PV-thermal (PVT) collectors to enhance their electrical efficiency and harness residual heat for supplementary purposes. Through computational fluid dynamics (CFD) simulations in Ansys-Fluent and Ansys Steady-state Thermal, an initial model is analyzed and optimized to develop three alternative models with improved electrical and thermal performance. The study focuses on varying geometrical aspects of the heat exchanger to evaluate their impact on defined Key Performance Indicators (KPIs), including pressure drop and fluid temperature gain. The results show that the increase in thermal efficiency may compromise homogeneous thermal flow distribution, emphasizing the need for a balance between thermal efficiency and uniform cooling distribution. This research provides valuable insights for optimizing thermal management designs in PV panel retrofit applications, contributing to advancing PV and PVT technologies and systems.

Keywords: Photovoltaics, Heat exchanger, Retrofitting, Computational fluid dynamics, Thermal management, Hybrid photovoltaic thermal (PVT) systems.

1. Introduction

Solar energy stands as a cornerstone within the realm of renewable energy, offering immense potential for sustainable power generation. Within the framework of photovoltaic (PV) cells, only a fraction of the incident solar radiation is directly converted into electrical energy. A significant portion of this solar irradiance is absorbed by the PV cells, leading to increased temperatures and subsequent reductions in panel efficiency and longevity. Recognizing the importance of mitigating this heat buildup, efforts have been directed towards the cooling of PV panels to enhance their electrical efficiency. In this regard, the cooling techniques explored so far can be classified into passive and active cooling mechanisms (Herrando et al. 2023). Passive cooling systems do not require additional power consumption to absorb the heat from PV panels. Heat pipes, phase change materials (PCMs), adding extended surfaces to the PV panel surface, among others are the commonly used passive cooling mechanisms. Alternatively, active cooling technologies use heat transfer fluids (HTFs) driven by external power-consuming devices like a fan or a pump to extract heat from the PV modules. One of the widely adopted active cooling strategies is the integration of thermal absorbers behind the PV panels, which gives rise to photovoltaic thermal (PVT) collectors.

PVT systems offer the dual benefits of generating thermal energy and electric power from the same aperture area thus making the renewable energy (RE) system more versatile (Chow, 2010 and Tripanagnostopoulos 2002). However, the effectiveness of the PVT system depends on how efficiently the heat energy can be absorbed. Among the various influencing factors, the design characteristics of the thermal absorber play a crucial role in determining the performance of the PVT system. Water-based PVT collectors are widely used as they are considered more efficient due to the high specific capacity of the heat transfer fluid. By water-based collectors, the authors also include water-glycol mixtures, one of the commonly used HTFs. Previous research has focused on the design and development of thermal absorbers for the water-based PVT collector, both in terms of the materials chosen and the overall geometrical specifications.

Various thermal absorber configurations have already been tested for PVT collectors. Among them, parallel

Selection and/or peer review under responsibility of Scientific Committee
10.18086/eurosun.2024.07.08 Available at http://proceedings.ises.org

tubes (pipes) are widely explored due to their geometrical simplicity (Herrando et al., 2014) that can achieve TRLs of 9. Due to this high TRL level, this configuration is also used for many commercial PVT collectors (Herrando et al., 2023). It has already been reported that, in this configuration, the thermal energy that can be extracted depends upon the W/D ratio (where W is the distance between the pipes and D is the pipe diameter), the collector fin efficiency, and the tube bonding quality (Herrando et al., 2023). These parameters are, therefore, considered to be directly influencing the efficiency of the collector. In this regard, several design optimization efforts have been reported in the literature by altering these parameters (Herrando et al., 2019). Huang et al., 2001 conducted studies using different thermal absorber materials, such as aluminium and copper with thermally conductive adhesive between the PV panel and the thermal absorber. From the analysis, it was found that the PVT system performance could have been more satisfactory. One of the other conclusions was that the absorber plate should be in direct contact with the PV cells to ensure proper heat transfer. Convective heat transfer between the coolant and the channels needs to be maximized to enhance the performance of the thermal absorber. This can be achieved by reducing the pipe diameter, D, and by increasing the number of channels per unit width (W) (Ji et al., 2006). Following this investigation, He et al., 2006 concluded that by using a flat-box design, the key design factors such as the collector fin efficiency and the tube-bonding quality could be further improved. This design was later explored by several authors in which the W/D ratio was reduced to 1 by using square channels (Huang et al. 2001). It was found that such a design could improve the fin efficiency by increasing the heat transfer area between the absorber plate and the cooling fluid. One of the outcomes of these studies was that to collect more than 90% of the energy, it was essential to have a fluid layer thickness smaller than 10 mm (Cristofari et al., 2002).

Among the materials used for the thermal absorber, copper is widely used owing to its high thermal conductivity (Makki and Sabir 2015, Michael and Goic 2015). However, one of the disadvantages of metal-based thermal absorbers is that the overall system weight and cost increase. This is not recommended considering the additional requirement of supporting structures that would increase the installation as well as the maintenance costs. This drawback arising from the material perspective, however, can be mitigated using a polymer-based thermal absorber that would significantly reduce the system weight and cost. Additionally, they offer a special advantage in terms of design, as they can acquire layouts that would be very difficult and expensive using conventional materials. Despite these advantages of using polymer-based material for thermal absorbers, only a few studies (Cristofari et al., 2002, 2009) so far have reported using polycarbonate material for thermal absorbers. Even though the effectiveness of current heat exchangers in absorbing thermal energy is already proven, they frequently encounter challenges in achieving homogeneous thermal distribution across the backside surface of the PV panel. This uneven thermal distribution heightens the risk of developing hotspots within the panel, leading to decreased electrical efficiency (Nahar et al., 2019). Researchers in this area have already demonstrated that innovative configurations, designs, and materials could increase the overall efficiency, cost-effectiveness, and reliability of PVT collectors (Herrando et al., 2019).

Despite the promising prospects of PVT technologies, their optimal design and competitiveness for effective heat extraction still need to be improved, hindering their widespread adoption. Nevertheless, there is a growing need to try out novel configurations other than that of the parallel pipe design. Therefore, The present study intends to develop a polymer-based thermal absorber; hence, the proposed geometrical specifications, primarily the fluid domain, are designed to ensure uniform thermal distribution and maximized heat absorption from the PV panel. The selection of polymeric material is also aimed at reducing manufacturing costs by taking advantage of the economy of scale in producing polymeric elements, as opposed to copper and aluminium heat exchangers. However, it is important to highlight that for a fair comparison with the existing configurations at this developmental stage, all studies of this work have been carried out considering aluminium as the material of choice.

2. Methodology

The methodology employed in this study involves an initial comparative analysis focusing on varying two key geometrical aspects in the thermal absorber: i) orifice sizing and ii) orifice spacing, to identify trends and understand how these parameters influence the defined key performance indicators (KPIs). This initial phase aimed to establish a foundational understanding of the impact of primary geometric modifications on system performance. The KPIs are defined in Section 2.1.

Following identifying these trends, the methodology progressed to iteratively refining a model focused on optimizing thermal power output. This iterative process incorporated additional geometrical features, such as baffles and different orifice arrangements, to enhance thermal performance. Building upon the insights gained from these iterations, three distinct models were ultimately proposed. The first model was optimized for maximum thermal power output, ensuring the highest possible thermal energy capture and heat transfer. The second model focused on achieving thermal homogeneity, ensuring uniform temperature distribution and minimizing thermal gradients in the PV module. The third model represented a trade-off design, balancing thermal power output and thermal homogeneity to provide a versatile and practical solution.

2.1. Key Performance Indicators (KPIs)

KPIs are needed to provide numerical insights that validate the hypotheses of each design modification in the optimization of the thermal absorber. KPIs serve as quantifiable measures that evaluate the performance and efficiency of different geometric configurations and therefore flow distributions. The indicators chosen in this study are pressure drop, temperature gain, thermal absorber wall temperature, internal heat transfer coefficient, Nusselt number, temperature standard deviation, thermal power, and thermal and electric efficiency.

Temperature gain (ΔT) refers to the increase in the fluid's temperature as it passes through the thermal absorber. It is a direct measure of the thermal power captured by the system and is essential for evaluating the efficiency of the heat exchanger. If the flow rate is kept constant, a higher temperature gain indicates better thermal performance, contributing to higher thermal energy production. This indicator helps determine the capacity of the design to efficiently absorb and transfer heat from the PV panel to the working fluid.

The thermal absorber wall temperature **(**T_{wall}**)** is an important KPI that reflects the average temperature on the surface of the absorber in contact with the photovoltaic panel. This temperature provides information about the thermal load experienced by the absorber material and the cooling potential of the PV cells. It is necessary to maintain a reduced wall temperature level to increase the durability and longevity of the thermal absorber. Excessively high wall temperatures can lead to material degradation, while low temperatures may indicate poor thermal energy production.

The internal convective heat transfer coefficient (h_{conv}) quantifies the heat transfer efficiency between the absorber surface and the working fluid. A higher convection value signifies more effective heat transfer, contributing to higher thermal power extraction and better overall system performance. The internal heat transfer coefficient is calculated with eq. 1.

$$h_{conv}[W\,m^{-2}K^{-1}] = \frac{q}{T_{wall}-T_m} \quad \text{(eq. 1)}$$

where $q\ [W\,m^{-2}]$ refers to the heat collected by the absorber and T_m refers to the average temperature of the fluid between the inlet and outlet.

The Nusselt number (Nu) is a dimensionless number that characterizes the ratio of convective to conductive heat transfer within the fluid. It provides an overall understanding of convective heat transfer relative to conduction. A higher Nusselt number indicates improved convective heat transfer, often achieved through design features that induce turbulence. It is calculated with eq. 2.

$$Nu = \frac{h_{conv}\,L}{k} = \frac{h_{conv}\,D_h}{k} \quad \text{(eq. 2)}$$

where D_h refers to the hydraulic diameter of the absorber and k refers to the thermal conductivity of the heat transfer fluid.

The temperature standard deviation (σ_T) measures the variation in temperature within the surface of the PV panel that is in contact with the thermal absorber. It is a crucial indicator of thermal homogeneity, as a lower deviation indicates a more uniform temperature distribution. Achieving a low standard deviation is necessary to avoid hot spots affecting PV electrical production and ensure uniform thermal performance throughout the absorber. This KPI helps identify designs that balance heat absorption and distribution, optimizing both electrical production by evenly cooling the cells and thermal performance. It is defined with eq. 3.

$$\sigma_T[K] = \sqrt{\frac{\sum_{i=1}^{N}(T_i-\overline{T})^2}{N}} \quad \text{(eq. 3)}$$

where T_i refers to the temperature of each cell, $\overline{T}$ refers to the mean temperature value of the cells, and *N* refers to the number of cells considered in each simulation.

Thermal power ($P_{th}[W\ m^{-2}]$) measures the amount of heat transfer from the absorber to the working fluid per unit collection area. It is a key indicator of the system's ability to convert solar energy into usable thermal energy. It is defined in eq. 4.

$$P_{th}[W_{th}\ m^{-2}] = \dot{m}\ C_p\ \Delta T\ \frac{1}{A_c} \qquad \text{(eq. 4)}$$

where $\dot{m}$ and C_p refer to the mass flow rate and the specific heat capacity of the fluid, respectively, and A_c refer to the area of collection of the PV panel.

Subsequently, thermal efficiency ($\eta_{th}[\%]$) represents the proportion of incident solar energy that is successfully converted into thermal energy by the system. It is a measure instantaneous thermal performance of the collector. Is is obtained with eq. 5.

$$\eta_{th}[\%] = \frac{P_{th}}{G} \qquad \text{(eq. 5)}$$

where $G\ [W\ m^{-2}]$ refer to the solar irradiance that in this case is used as a contant heat flux boundary condition.

The parameters that relate electrical production with thermal performance are the photovoltaic efficiency ($\eta_{el}[\%]$), which describes how the efficiency of the PV panel changes with temperature and the electrical power production per unit area of collection $P_e\ [W\ m^{-2}]$. Their relationship is given by the following eq. 6 and eq. 7.

$$\eta_{el}[\%] = \eta_{PV,ref}\left[1 + \beta_0\left(T_{PV} - T_{PV,ref}\right)\right] \qquad \text{(eq. 6)}$$

$$P_{el}[W_{el}\ m^{-2}] = G\ \eta_{el} \qquad \text{(eq. 7)}$$

where $\eta_{PV,ref}$ refers to the reference PV efficiency at the reference temperature, β_0 is the temperature coefficient of the PV cells, T_{PV} refers to the temperature of the PV cells and $T_{PV,ref}$ refers to the reference temperature of the PV panel, equal to 298 K.

Lastly, the pressure drop is a critical indicator that measures the resistance encountered by the fluid as it flows through the thermal absorber. Therefore, it is indicative of the energy required to maintain fluid circulation, directly impacting the pumping power requirements of the system. The pressure drop characterization is commonly presented as a function of the flow rate in the thermal absorber. A lower pressure drop ($\Delta P[Pa]$) is desirable as it implies lower energy consumption for fluid movement, enhancing overall system efficiency and reducing initial investments.

2.2. CFD and Steady-State Thermal models.

For the geometrical design of the PVT retrofit, multiple CFD models were developed, enabling a detailed study of various aspects of fluid flow and heat transfer within the collector. The following sections present these models along with their underlying rationale: i) Half-retrofit model (fluid only), ii) Half-retrofit model with PV layer, and iii) Half-PV panel model.

2.3.1. Half-retrofit model (fluid only)

The half-retrofit models (fluid only) are used primarily to optimize the flow distribution of the designs. These models do not consider the attachment of any PV panel and the conversion of electricity in the heat flux boundary condition. The aim is to examine the trends of the flow under different geometry variations. The boundary conditions for these models are specified in Tab. 1. The material selected is aluminium for comparative purposes with thermal absorber geometries presented in the literature.

Tab. 1: Boundary conditions for the fluid flow in Fluent.

Fluid - Material	Water - Aluminium
Fluid flow-rate	0.035 kg/s
Pressure inlet	3 bar

Temperature inlet	293 K
Fluid domain thickness	6 mm
Solar irradiance / Heat flux	1000 W/m^2

2.3.2. Half-retrofit model with PV layer

The half-retrofit model with the PV layer involves a system coupling simulation using ANSYS Fluent and Steady-State Thermal modules. This model aims to calculate the nominal values of the PVT collector retrofit when operating under realistic conditions, such as electric and thermal power. The electrical properties of the PV panel taken as reference are 300 W_{el} of peak electrical power, 18.44% for the nominal PV cell efficiency, -0.39 %/K as power temperature coefficient, and 1.62 m^2 as gross area, representing a conventional c-Si PV panel. The thermal properties of the PV panel layers used as a reference in these simulations are presented in Tab. 2. These properties were introduced into the model as a single layer, using a weighted average value based on the thickness of each layer.

Tab. 2: PV panel layers properties considered.

Layer	Specific heat [J/kg K]	Density [kg/m3]	Conductivity [W/mK]	Thickness [mm]
Tempered Glass	779.70	2125	1.15	3.00
EVA (x2)	2098	950	0.35	0.50
Solar Cells (c-Si)	702	2330	124	0.26
TEDLAR	1200	1765	0.17	0.10

The boundary conditions for Fluent remain the same as in the fluid-only models, except for the heat flux value (reduced to consider the conversion of energy into electricity) and surface application, as mentioned in the previous section. Additionally, Tab. 3 presents the boundary conditions used for the Steady-State Thermal module, including convection and radiation losses characterized by the heat transfer coefficients. These boundary conditions are consistent with those established in reviewed studies from the literature (Herrando et al., 2023), aiming for the simulation results to be compared accordingly.

Tab. 3: Steady-state thermal boundary conditions.

Solar Irradiance / Heat flux	1000 W/ m^2
Ambient Temperature	25 ºC
Convective Heat Transfer Coefficient (Front)	4.79 W/ m^2 K
Convective Heat Transfer Coefficient (Back)	0.45 W/ m^2 K
Emissivity of Glass	0.86
Emissivity of Solar PV Cells	0.89

The electrical conversion consideration process begins by applying a Solar Irradiance of 1000 W/m² to determine the PV cell temperature. Once the PV cell temperature is determined, the corrected efficiency of the PV cells at this temperature is calculated with eq. 6. The calculated electrical efficiency is then subtracted from the initial 1000 W/m² solar irradiance to estimate the remaining heat flux available for the thermal conversion. This adjusted heat flux value is subsequently used to run the final simulation, providing a more accurate representation of the system's thermal behaviour after accounting for the electrical energy extracted by the PV module.

2.3.3. Half-PV panel model

The half-PV panel model is a Steady-State Thermal model in ANSYS, similar to the previous steady-state thermal model without including the Fluent part. This model considers only the PV panel layers without the heat exchanger and the fluid domain, serving as a reference to determine the temperature of the PV cells and

electrical efficiency without any cooling effect. It is used to compare the electrical performance improvements achieved by integrating the heat exchanger in the previous models.

3. Optimization towards energy production

Before delving into the optimization towards energy production, it is essential to address a key design consideration that significantly affects the overall configuration of the thermal absorber. It has been decided to split the model into two halves to overcome the problem posed by the junction boxes of next-generation PV panels. Modern PV panels, particularly those using medium-sized solar cells, are equipped with three junction boxes at the back. These junction boxes can obstruct the placement of the heat absorber and affect the heat transfer efficiency. Therefore, dividing the model into two identical sections allows the heat absorber to be placed above and below the junction boxes, ensuring an unobstructed path for heat transfer (see Fig. 1, right). This configuration allows the absorber to be connected without passing through the junction boxes. This strategic decision lays the foundation for the subsequent detailed optimization of energy production, ensuring effective management of the practical challenges of the installation. Fig. 1 shows a rendering of a conventional PV panel with three junction boxes and the possible configuration for the split retrofit.

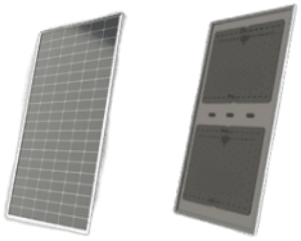

Fig. 1: Conventional PV panel and the possible configuration for the split retrofit.

3.1. Influence of flow distribution on thermal production

In this section, the influence of the flow distribution on the thermal output within the heat exchanger of the solar collector is discussed in more detail. The main objective is to improve the KPI related to the temperature gain. Firstly, a comparative approach is adopted, using half-collector (fluid only) simplified models with variations in the size and number of orifices, establishing the identified trends as a basis for developing the proposed orifice arrangements to maximize the temperature gain.

The simplified models (half collector and fluid only) present different orifice sizes (20 mm, 30 mm, 40 mm) and spacing, leading to different numbers of holes per row (3/4, 5/6, 7/8). For the different orifice sizes, an orifice spacing relative to 5/6 holes per row is considered, and on the other hand, for the different orifice spacing cases, an orifice size of 30 mm is considered. CFD simulations of these models have been carried out under the boundary conditions explained above, allowing trends to be observed and conclusions to be drawn on their impact on thermal output.

Tab. 4: Results of geometrical aspects and correlation of KPIs for thermal production (half collector, fluid only).

Model	T_1[K]	T_2[K]	$\Delta T[K]$
20 mm	293	303.3	10.3
30 mm	293	300.9	7.9
40 mm	293	298.4	5.4
3/4	293	302.3	9.3
5/6	293	299.7	6.7
7/8	293	298.1	5.1

The results presented in Tab. 3 show that reducing the size and number of holes benefits thermal output. Subsequently, based on the identified trends, an iterative adjustment of the hole layout is made to improve the temperature gain further, resulting in the optimal design to increase thermal output. Tab. 5 presents a description of the variations in the arrangement of the holes that were introduced to increase the temperature

gain and, therefore, the thermal production, taking as a basis a version (v1) that emulated the geometry of the original heat exchanger but with the hypothesis of a reduction in the size and number of holes introduced. It should be noted that the bridge between modules is a bypass with a height of 50 mm and a distance of 70 mm, which could be optimized to reduce the pressure drop and is excluded from this study.

Tab. 5: Description of the geometrical variations from v1 to v6 and results of the temperature gain for thermal production.

Model	Modifications with respect to the previous model	$\Delta T[K]$
v1	-	6.6
v2	Centred inlets and outlets (non-diagonal flow) to reduce the distance to opposite corners to be filled.	8.7
v3	Inclusion of a zone of high flow resistance in the centre, condensing the distance between holes locally, to create a tendency for the flow to avoid this zone and fill in the corners.	8.9
v4	Adjustment of the approximation of this zone to the inlet.	10.3
v5	Inclusion of flaps and a deflector at the outlet to improve the reach in the corners.	10.7
v6	Lengthening of the deflector to maximise corner outreach.	12.1
v7	Adaptation of the deflector to reduce pressure drop.	13.9

After analyzing the flow behaviour of each version, it is possible to identify the optimal orifice arrangements that maximize the temperature gain while maintaining or improving other critical KPIs and to propose a design oriented towards thermal production (Design A). Fig. 2 shows the first version (v1) and the final developed design (v7 – Design A), aimed at maximizing thermal output. Consequently, Fig. 3 shows a rendering of Design A, developed following these considerations (left), alongside its temperature field in a plane in the middle of the fluid domain (right). Moreover, the numerical results obtained regarding thermal output and their improvement with respect to the first conceptualized version are a temperature gain ($\Delta T[K]$) enhancement from 6.6 K in v1 to 13.9 K.

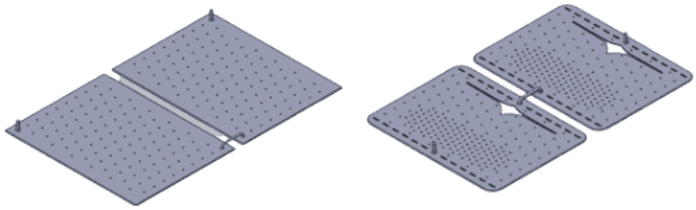

Fig. 2: First version (v1) and the final developed design (v7), aimed at maximizing thermal output.

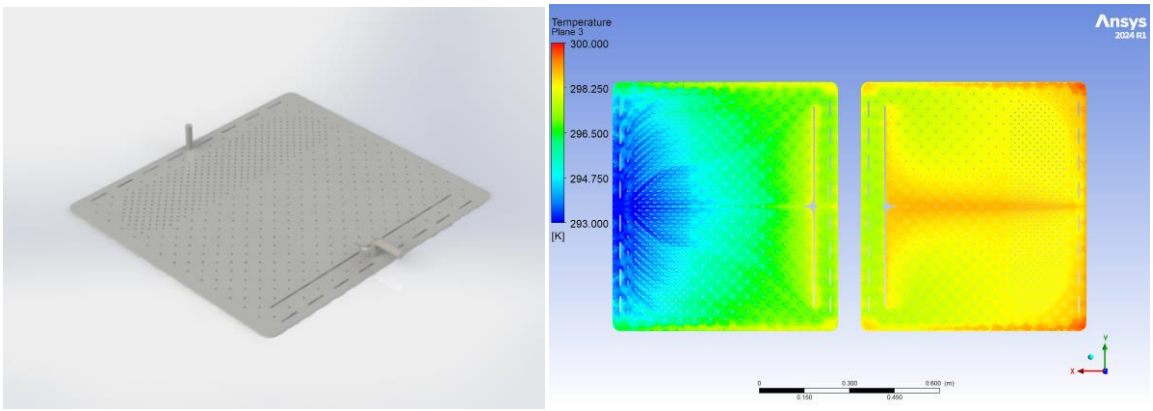

Fig. 3: Rendering of Design A (left), and its temperature field (right).

3.2. Influence of flow distribution on electrical production

The influence of the flow distribution on the electrical output is an important aspect of the design optimization process; the main objective in this respect is to reduce the wall temperature of the heat absorber, thus lowering

the operating temperature of the PV panel. This is essential because PV cells exhibit higher efficiency at lower temperatures, and minimizing their operating temperature can significantly improve the overall electrical output of the system.

To achieve this goal, the focus is on maximizing the Nusselt number and the convective heat transfer coefficient. These parameters are directly related to the efficiency of heat transfer from the absorber surface to the fluid. Higher values indicate more efficient cooling, which helps maintain lower temperatures for the PV panels.

One of the most effective ways to increase the Nusselt number and convection coefficient is to ensure a high fluid flow velocity and, therefore, increase the Reynolds number. A high flow velocity improves convective heat transfer, leading to more uniform and efficient cooling over the entire absorber surface. To achieve higher flow velocities, the design must incorporate reduced orifice spacing, facilitating a more turbulent and faster-moving fluid flow. Nevertheless, given the geometry, this becomes a trade-off against the amount of available surface for heat transfer and, thus, thermal output, as well as a tentative increase in pressure drop in the absorber. In this sense, Fig. 4 shows a rendering of Design B, developed following these considerations (left), alongside its temperature field in a plane in the middle of the fluid domain (right).

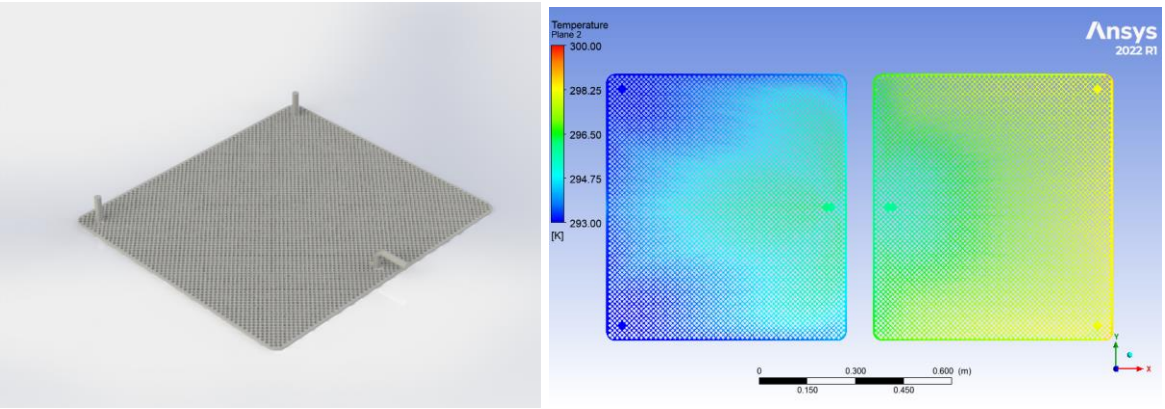

Fig. 4: Rendering of Design B (left), and its temperature field (right).

4. Optimization analyses

4.1 Identification of optimal geometric configurations

To propose a design that meets a coherent compromise between thermal power generation and electrical efficiency enhancement, iterative simulations and evaluations of different geometrical configurations are carried out. The aim is to identify a design that offers an acceptable compromise between maximum possible output temperature, thermal homogeneity and reduced pressure drop. This involves adjusting parameters such as orifice spacing and orifice arrangement. As explained in previous sections, smaller orifices with reduced orifice spacing can increase flow velocity and improve convective heat transfer alongside thermal homogeneity, leading to better cooling and lower wall temperatures, resulting in lower cell operating temperatures and, hence, higher electricity production from the panel attached to the heat exchanger.

However, this configuration may result in higher pressure drops and lower thermal output due to limited fluid flow. An optimized layout that ensures uniform flow distribution can help achieve thermal homogeneity and efficient heat transfer. In this regard, incorporating an accumulation zone at the inlet and outlet, alongside a discontinuous baffle, can effectively distribute the fluid evenly, minimize overheating zones, and ensure efficient heat extraction. This design induces a flow path that minimizes dead zones at corners and ensures uniform fluid movement over the entire surface of the heat exchanger, prioritizing. Analyzing the trends obtained in Section 3.1 about orifice dimensions and orifice spacing, Tab. 6 presents the main geometric considerations taken in this regard for the third and rest of the proposed designs. Fig. 5 shows a rendering of Design C proposed heat exchanger, together with the temperature map, where the objective is developing a model with an intermediate approach between wall cooling and thermal energy development. In turn, Tab. 7 presents the CFD results and compares them to the other models focused on different energy generation previously developed.

Tab. 6: Geometric considerations for the three proposed designs.

Parameter	Design A	Design B	Design C
Orifice size [mm]	5	9	7
Orifice spacing [mm]	50	15	20

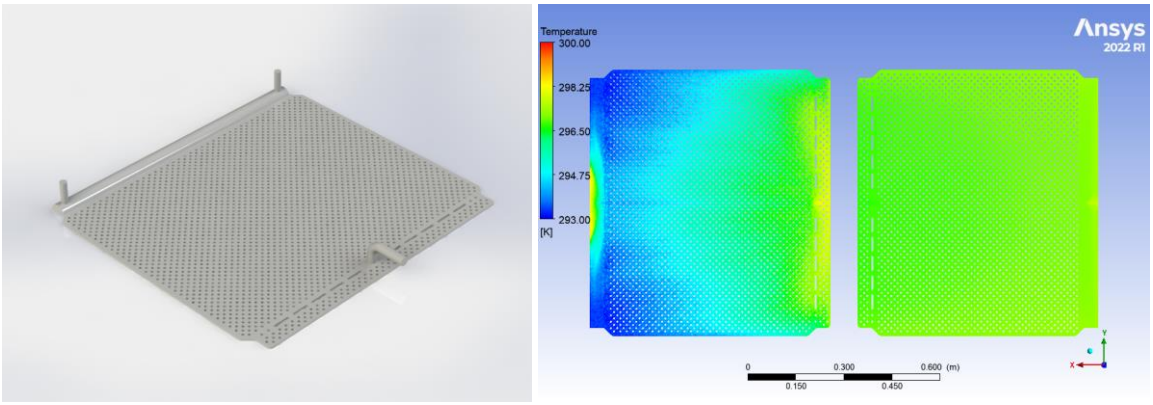

Fig. 5: Rendering of Design C (left), and its temperature field (right).

Tab. 7: CFD results performed on the three models.

Parameter	Design A	Design B	Design C
ΔT **[K]**	6.9	5.1	4.2
T_{wall} **[K]**	299.2	296.7	297.5
h_{conv} **[W m^{-2} K^{-1}]**	181.9	324.2	615.8
Nu	3.2	5.9	11.3
σ_T **[K]**	1.6	1.5	1.2
P_{th} **[W m^{-2}]**	604.8	450.2	372.2
η_{th} **[%]**	60	45	37
T_{PV} **[K]**	299.8	296.8	297.6
P_{el} **[W m^{-2}]**	183.1	185.3	184.7
η_{el} **[%]**	18.3	18.5	18.4
ΔP **[Pa]**	72	271	36

Tab. 8: Steady-State Thermal results for the half-PV panel model without cooling.

Parameter	Half-PV panel model
P_{el}**[W m^{-2}]**	144.1
η_{el}**[%]**	14.4
T_{PV}**[K]**	364.1

In addition, through multiparametric analysis, the pressure drop curve against flow rate was determined for Design A. Fig. 6 presents the curve, illustrating how increasing the flow rate leads to a corresponding rise in pressure drop. Given the similar geometric configurations and fluid dynamics principles applied across the other designs, it is expected that the pressure drop behaviour for these designs will follow a similar trend.

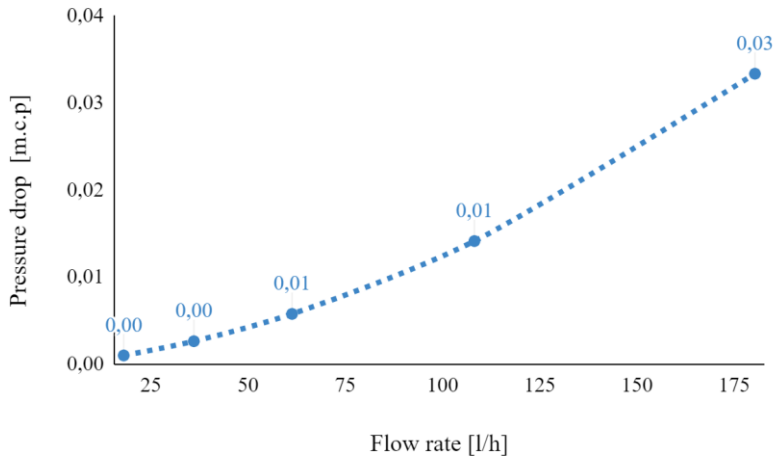

Fig. 6: Flow rate vs. Pressure drop for Design A.

4.2. Comparative analysis with different proposed configurations.

Three different designs were proposed for the polymeric heat exchanger to convert a PV panel into a PVT retrofit. The designs were tailored to address distinct objectives: enhancing electrical output by cooling the PV panel, maximizing thermal power generation, and a balanced trade-off design that aims to achieve both goals. The analysis evaluates each design's performance, providing insights into their suitability based on varying user demand profiles for electricity and heat. For the study, a conventional PV panel of 300W_{el} is chosen as a reference. Fig. 6 shows a visual comparison (not to scale) of CFD results between the different designs developed.

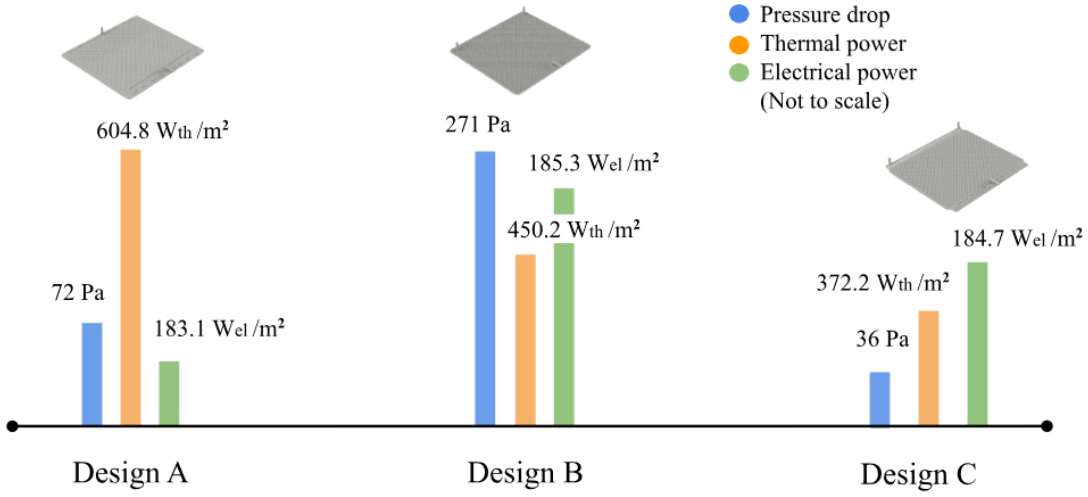

Fig. 7: Visual comparison (not to scale) of CFD results between the developed designs.

Design A focuses on maximizing thermal energy generation. This design features modifications that optimize the heat exchanger's performance in transferring solar thermal energy to the working fluid, enhancing the system's overall thermal output. The increased electrical output of this design is calculated as +21.3% compared to a PV-only panel, with a thermal power development of 604.8 W_{th} and a pressure drop of 72 Pa. This makes Design A suitable for applications where the primary demand is for heat, such as domestic hot water or low-grade industrial process heat.

On the other hand, Design B incorporates smaller flow channels by reducing orifice spacing to maximize the convective heat transfer coefficient and Nusselt values, which increases the cooling effect on the PV cells. This significantly reduces the PV cell temperature, leading to a noticeable relative improvement in electrical efficiency by up to +22.2%, compared to a PV-only panel. The design develops a thermal power output of 450.2 W_{th} and has a pressure drop of 271 Pa. The reduction in temperature correlates with an increase in electrical production, making this design ideal for scenarios where the primary demand is for electricity.

However, deeper analysis is needed to address the pressure drop and pumping requirements.

Lastly, Design C was initially conceived as an intermediate option between Design A and Design B, intending to balance the cooling of the PV panel and the generation of thermal energy. Although it was expected to be closer in performance to Design B due to similar orifice size and spacing, the inclusion of an accumulation zone in Design C led to a notable reduction in pressure drop. This adjustment resulted in a model with a significantly lower pressure drop (38 Pa) while achieving less thermal output (372.2 Wth /m^2) but similar electrical efficiency to those of Design B (184.7 Wth /m^2), representing an increased +21.7% electrical efficiency compared to a PV-only panel.

5. Discussion and conclusions

This study conducted an extensive comparative analysis of various geometrical configurations for a thermal absorber, focusing on KPIs such as pressure drop, temperature gain, thermal absorber wall temperature, convective heat transfer coefficient, Nusselt number, temperature standard deviation, thermal power, and electrical efficiency. The initial phase involved examining orifice sizing and spacing to identify performance trends. Based on these insights, a model was iteratively refined to optimize thermal power, proposing two additional models: one emphasizing thermal homogeneity and another balancing pressure drop reduction and homogeneity. The findings provide a comprehensive understanding of how geometric modifications affect absorber performance, guiding future design improvements. The results demonstrated an electrical enhancement of approximately +21.3%, +22.2% and +21.7% compared to the PV-only panel before retrofitting this solution into PVT systems. Additionally, the system provided a substantial energy surplus in the form of low-grade hot water, showing thermal efficiencies of 60%, 45% and 37%, representing thermal energy outputs of 604.8 W/m^2, 450.2 W/m^2, and 372.2 W/m^2 across the three different configurations. This thermal power development and electrical efficiency enhancement are two aims that could be tackled in the design phase and that depend on the user's specific needs. The choice between these designs should be guided by the particular user demand profile. Users with a higher electricity demand may prefer the electrical enhancement designs, as they maximize the PV panel's electrical efficiency. Conversely, users requiring more thermal energy should opt for the thermal power development design, which excels in heat generation.

Future work will explore further optimization of these models under varying operational and physical conditions, such as the integration of advanced polymeric materials or nanofluids as heat transfer fluid to enhance overall system efficiency, and experimental validation utilizing prototyping.

6. Acknowledgments

This study has been developed under the framework of the PVT4EU project, granted by the Clean Energy Transition Partnership Programme (project ID. CETP-2022-00403). The work is supported by national funds through Sweden: Swedish Energy Agency (P2023-00884); Denmark: Innovation Fund Denmark (3112-00010B); and Portugal: FCT- Fundação para a Ciência e a Tecnologia, I.P. This work is also supported by Spanish funds in the framework of the Juan de la Cierva Incorporación Fellowship awarded to Dr. María Herrando, funded by the Ministry of Science, Innovation and Universities (AEI) and cofounded by the EU (through the NextGeneration funds) [grant number IJC2020-043717-I].

The study was also supported by the Swedish Energy Agency (grant number 2021-036454)

7. References

Agathokleous, R.A., Ding, Y., Ekins-Daukes, N., Herrando, M., Huang, G., Kalogirou, S., Markides, C.N., Mousa, O.B., Otanicar, T., Taylor, R.A., Wang, K., 2023. A review of solar hybrid photovoltaic-thermal (PV-T) collectors and systems. *Progress in Energy and Combustion Science* 97, 101072. https://doi.org/10.1016/j.pecs.2023.101072

Chow, T.T., 2010. A review on photovoltaic/thermal hybrid solar technology. *Applied Energy* 87, 365–379. https://doi.org/10.1016/j.apenergy.2009.06.037

Cristofari, C., Notton, G., Canaletti, J.L., 2009. Thermal behavior of a copolymer PV/Th solar system in low flow rate conditions. *Solar Energy* 83, 1123–1138. https://doi.org/10.1016/j.solener.2009.01.008

Cristofari, C., Notton, G., Poggi, P., Louche, A., 2002. Modelling and performance of a copolymer solar water heating collector. *Solar Energy* 72, 99–112. https://doi.org/10.1016/s0038-092x(01)00092-5

Fudholi, A., Sopian, K., Yazdi, M.H., Ruslan, M.H., Ibrahim, A., Kazem, H.A., 2014. Performance analysis of photovoltaic thermal (PVT) water collectors. *Energy Conversion and Management* 78, 641–651. https://doi.org/10.1016/j.enconman.2013.11.017

Guarracino, I., Freeman, J., Ramos, A., Kalogirou, S.A., Ekins-Daukes, N.J., Markides, C.N., 2019. Systematic testing of hybrid PV-thermal (PVT) solar collectors in steady-state and dynamic outdoor conditions. *Applied Energy* 240, 1014–1030. https://doi.org/10.1016/j.apenergy.2018.12.049

He, W., Chow, T.-T., Ji, J., Lu, J., Pei, G., Chan, L.-S., 2006. Hybrid photovoltaic and thermal solar-collector designed for natural circulation of water. *Applied Energy* 83, 199–210. https://doi.org/10.1016/j.apenergy.2005.02.007

Herrando, M., Hellgardt, K., Markides, C.N., 2014. A UK-based assessment of hybrid PV and solar-thermal systems for domestic heating and power: System performance. *Applied Energy* 122, 288–309. https://doi.org/10.1016/j.apenergy.2014.01.061

Herrando, M., Markides, C.N., Huang, G., Otanicar, T., Mousa, O.B., Agathokleous, R.A., Ding, Y., Kalogirou, S., Ekins-Daukes, N., Taylor, R.A., Wang, K., 2023. A review of solar hybrid photovoltaic-thermal (PV-T) collectors and systems. *Progress in Energy and Combustion Science* 97, 101072. https://doi.org/10.1016/j.pecs.2023.101072

Herrando, M., Ramos, A., Zabalza, I., Markides, C.N., 2019. A comprehensive assessment of alternative absorber-exchanger designs for hybrid PVT-water collectors. *Applied Energy* 235, 1583–1602. https://doi.org/10.1016/j.apenergy.2018.11.024

Huang, B.J., Lin, T.H., Hung, W.C., Sun, F.S., 2001. Performance evaluation of solar photovoltaic/thermal systems. *Solar Energy* 70, 443–448. https://doi.org/10.1016/s0038-092x(00)00153-5

Ibrahim, A., Othman, M.Y., Sopian, K., Ruslan, M.H., Alghoul, M.A., Yahya, M., Zaharim, A., 2009. Performance of photovoltaic Thermal collector (PVT) with different absorbers design. **WSEAS Transactions on Environment and Development 5, 321–330.**

Makki, A., Omer, S., Sabir, H., 2015. Advancements in hybrid photovoltaic systems for enhanced solar cells performance. *Renewable & Sustainable Energy Reviews* 41, 658–684. https://doi.org/10.1016/j.rser.2014.08.069

Michael, J.J., S, I., Goic, R., 2015. Flat plate solar photovoltaic–thermal (PV/T) systems: A reference guide. *Renewable & Sustainable Energy Reviews* 51, 62–88. https://doi.org/10.1016/j.rser.2015.06.022

Nahar, A., Hasanuzzaman, M., Rahim, N.A., Parvin, S., 2019. Numerical investigation on the effect of different parameters in enhancing heat transfer performance of photovoltaic thermal systems. *Renewable Energy* 132, 284–295. https://doi.org/10.1016/j.renene.2018.08.008

Tripanagnostopoulos, Y., Nousia, Th., Souliotis, M., Yianoulis, P., 2002. Hybrid photovoltaic/thermal solar systems. *Solar Energy* 72, 217–234. https://doi.org/10.1016/s0038-092x(01)00096-2

Xu, P., Zhang, X., Shen, J., Zhao, X., He, W., Li, D., 2015. Parallel experimental study of a novel super-thin thermal absorber based photovoltaic/thermal (PV/T) system against conventional photovoltaic (PV) system. *Energy Reports* 1, 30–35. https://doi.org/10.1016/j.egyr.2014.11.002